

Supporting Information for

Quorum Sensing Communication Between Lipid-Based Artificial Cells

Antoni Llopis-Lorente,^{ab} Bastiaan C. Buddingh',^a R. Martínez-Máñez,^b Jan C. M.
van Hest*^a and Loai. K. E. A. Abdelmohsen*^a

^a*Department of Chemical Engineering and Chemistry, Department of Biomedical Engineering,
Institute for Complex Molecular Systems &, Eindhoven University of Technology, PO Box 513,
5600 MB Eindhoven, the Netherlands. E-mail: J.C.M.v.Hest@tue.nl;
L.K.E.A.Abdelmohsen@tue.nl.*

^b*Instituto Interuniversitario de Investigación de Reconocimiento Molecular y Desarrollo
Tecnológico (IDM), Universitat Politècnica de València, Universitat de València, Spain; CIBER
de Bioingeniería, Biomateriales y Nanomedicina, Instituto de Salud Carlos III.*

Materials

1,2-dioleoyl-*sn*-glycero-3-phosphocholine (DOPC), 1-palmitoyl-2-oleoyl-glycero-3-phosphocholine (POPC), 1,2-distearoyl-*sn*-glycero-3-phosphoethanolamine-*N*-[biotinyl(polyethylene glycol)-2000] (DSPE-PEG), and 1,2-dioleoyl-*sn*-glycero-3-phosphoethanolamine-*N*-(lissamine rhodamine B sulfonyl) (DOPE-RhB) were provided by Avanti Polar Lipids. Paraffin oil (0.86 g/cm³ at 20 °C) was obtained from JT Baker. Cholesterol, glucose, sucrose, sodium chloride, urea, urease from *Canavalia Ensiformis* (Type III, 38 U/mg), bovine serum albumin (BSA), and phosphate buffer saline pills were purchased from Sigma-Aldrich. Green fluorescent protein (GFP) (M_w=29 kDa) was synthesized by recombinant expression in BL21(DE3) bacterial cells, as previously described.¹ Dextran-fluorescein-tetramethylrhodamine (dextran-RhB-FITC) conjugate (70,000 g/mol, anionic) was obtained from Thermo Fisher Scientific. DNA was synthesized and purified (HPLC) by Integrated DNA Technologies (Germany). The specific pH-responsive DNA nanoswitch sequence was as follows (adapted from Sánchez *et al.*)²:

5'-TTTTTTGAAGAAGGAATTT(Cy3)ATTCCTTCTTCGTTTGCTTCTTCCTT(Cy5)-3'

All other reagents and solvents were of high-quality grade, purchased from commercial suppliers, and used without further purification. Ultrapure water ("Milli-Q") was obtained from a Merck Millipore Q-Pod system (≥ 18.2 M Ω) with a 0.22 μ m Millipore Express 40 filter. Chambered microscope slides (18 wells, glass bottom) and channel slides (μ -slide VI 0.5 glass bottom) were purchased from Ibidi.

Instrumentation

Confocal laser scanning microscopy was performed using a Leica TCS SP5X or a Leica TCS SP8. Bulk fluorescence spectroscopy measurements were carried out using a Tecan Safire 2 plate reader. pH measurements were conducted using a FiveEasy Plus FEP20 pH meter (Mettler Toledo). Micrograph images were quantified and processed with Fiji, a program developed by the NIH and available as public domain software at <https://imagej.net/Fiji>.

Assembly of giant unilamellar vesicles (GUVs)

Our protocol for the preparation of GUVs is based on the droplet transfer method.³ Lipid stock solutions were prepared in chloroform and stored at -20 °C until use. Lipid solution aliquots were taken and mixed with 200 μ L of paraffin oil to obtain a lipid mixture (10 mM) containing DOPC, POPC and cholesterol in a molar ratio of 35/35/30.

For preparing pegylated liposomes, 1% of DSPE-PEG was added as well. When membrane labelling was needed, 0.06% DOPE-RhB was incorporated. Firstly, the lipid mixture in paraffin was heated at 80 °C for 30 min and cooled on ice for at least 15 min. Next, 20 µL of inner phase solution (*vide infra*) was emulsified in 200 µL of lipid solution by strong vortexing for 25 s while turning the reaction tube to prevent sedimentation of the water droplet. Directly after, the emulsions were incubated on ice for 10 min. Subsequently, they were layered on top of 150 µL of pre-cooled outer phase solution (10 mM acetate buffer, 150 mM NaCl, 200 mM glucose, pH 5) in a 1.5 mL plastic tube and immediately centrifuged at 4 °C for 20 min at 3300 rcf. GUVs were harvested by puncturing the tube at the position of the GUV pellet and collecting the dripping aqueous phase. To remove any non-encapsulated material, GUVs were washed by centrifugation at 1500 rcf for 2 min and replacement of the supernatant with 40 µL fresh outer phase, which was repeated twice.

Inner phase compositions: 10 mM acetate buffer, 150 mM NaCl, 200 mM glucose, pH 5. Where applicable, calcein was added at 10 µM, urease was added at 140 U/mL, GFP was added at 10 µg/mL, DNA was added at 10 µM, dextran-RhB-FITC was added at 100 µg/mL. All components were added from concentrated stock solutions.

Confocal laser scanning microscopy (CLSM) experiments

For microscopy experiments, GUVs were transferred into an 18-well µslide with a #1.5 glass coverslip bottom (Ibidi). Previously, the corresponding observation chamber was passivated by incubation with BSA (1 mg/mL) for at least 30 min and subsequently washed with Milli-Q water. GUV imaging by CLSM was performed on a Leica TCS SP5X equipped with a white light laser, using a HCX PL APO CS 63x/1.20 water-immersion objective and HyD detectors. 2x line averaging was applied. The image resolution was 1024 × 1024 pixels and scanning speed was 400 Hz. DOPE-RhB and GFP were imaged using sequential scanning. DOPE-RhB was excited at 555 nm and emission was collected at 570-615 nm; GFP was excited at 488 nm and emission was collected at 500-550 nm. DNA was excited at 530 nm and emission was simultaneously recorded at 550-620 nm (Cy3) and 640-715 nm (Cy5). For the kinetics experiments (Fig. 5a), FITC was excited at 488 nm and emission was collected at 500-540 nm; RhB was excited at 555 and emission was recorded at 570-615 nm, using HCX PL APO CS 20.0/0.70 dry objective. FITC and RhB were imaged each 10 min, with sequential excitation. For channel imaging (Fig. 5c and S7), CLSM was performed on a Leica TCS SP8, using a HC PL APO CS2 10x/0.40 dry objective and a HyD

detector. FITC was excited using a 488 nm laser, and emission was recorded at 495-535 nm; RhB was excited using a 552 nm laser, and emission was recorded at 565-610 nm, with sequential imaging. Calcein-loaded GUVs (Fig. S3) were imaged using the Leica TCS SP8, with a HC PL APO CS 20.0/0.70 dry objective. In all cases, settings were fixed during the experiments to allow direct comparison of the fluorescence intensities.

In a typical experiment, a batch of GUVs was divided into several aliquots at the corresponding dilution factors (5-, 50-, 100- or 500-fold dilution for quorum experiments; by taking 0.1, 0.5, 1, and 10 μL from the GUV stock, respectively; referred as population density (PD) of 0.2, 0.02, 0.01 and 0.002, respectively). The final volume was adjusted to 50 μL by addition of fresh outer phase (10 mM acetate buffer, 150 mM NaCl, 200 mM glucose, pH 5). GUVs were let to settle in the microscope chamber for at least 5 min before urea (at the corresponding concentration, from a concentrated stock) or ammonia (5 mM) were added. Samples were incubated for 3 h in the presence or in the absence of urea before imaging.

For kinetics experiments (Figure 5a), 10 μL of GUV stock were carefully placed with a pipette at the center of the microscope chamber (containing 40 μL of outer phase, with 25 mM urea final concentration). Images were acquired at the edge of the GUV cluster.

For experiments with the channel device, channels were loaded with 1 mg/mL BSA solution in Milli-Q and incubated for 1 h to passivate the surfaces. To remove the BSA solution, the channels were washed twice with Milli-Q and once with outer phase solution. Then, 160 μL of a solution containing 3 μL of GUV stock and 25 mM urea were loaded into the channel. Subsequently, 10 μL of GUV stock was deposited at the bottom of one of the reservoirs (total reservoir volume 50 μL , GUV PD=0.2, see schematic in Figure 5b), while 10 μL of outer phase were gently added in the other reservoir. The channel was let to incubate for 12 hours, followed by imaging using a 10x objective.

Spectroscopic characterization of the pH-responsive DNA nanostructure

The emission spectra of the pH-responsive DNA nanostructure showed in Fig. 3b was obtained by measuring aliquots of DNA in bulk solution (500 nM) in PBS (1X) adjusted at the corresponding pH. Excitation wavelength was 530 nm. Bulk fluorescence spectroscopy measurements were carried out using a Tecan Safire 2 plate reader. The ratiometric FRET values at different pH showed in Fig. 3c was calculated as $F_{\text{Cy5}}/(F_{\text{Cy3}} +$

F_{Cy5}); where F_{Cy5} is the maximum fluorescence emission of Cy5 ($\lambda_{em}=660$ nm) and F_{Cy3} ($\lambda_{em}=563$ nm).² Results are expressed as mean \pm standard deviation from 2 different samples.

Image analysis

Micrographs were analyzed using Fiji (ImageJ) applying standard functions. Vesicle diameter was calculated from the area extracted using the built-in particle analysis tool. To quantify the fluorescence output, individual GUVs were automatically selected as region of interest (ROI's) by thresholding the image and converting it into a binary image. The watershed function and manual selection tool were applied when necessary to distinguish GUVs in close proximity. Fluorescence intensities were extracted from the raw images (split channels) using the previously determined vesicle positions (ROI's) and plotted.

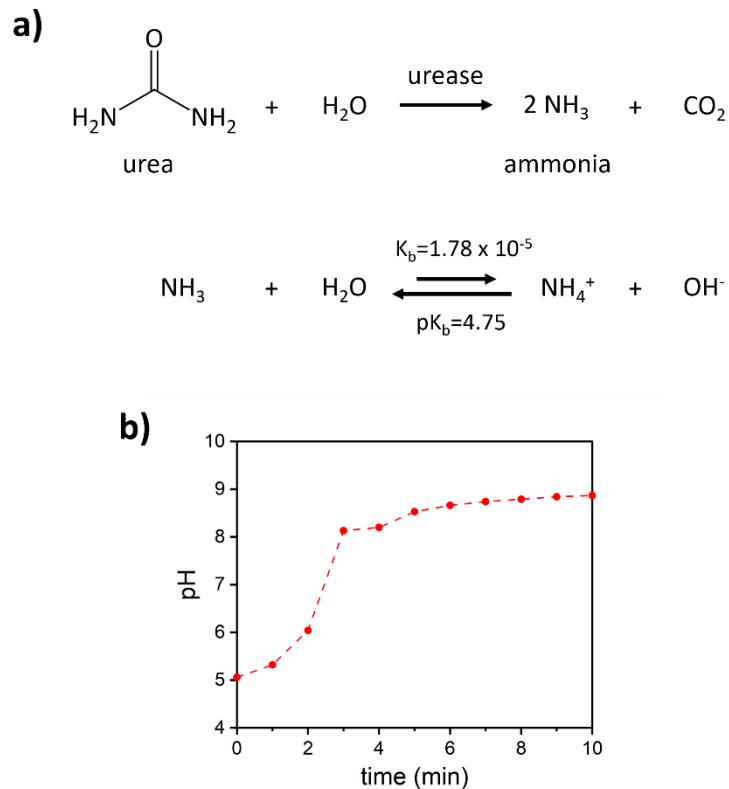


Fig. S1 Urease-mediated urea hydrolysis. a) Set of reactions involving the production of ammonia. b) The enzymatic reaction leads to an increase of pH over time. pH response a function of time in a solution initially set at pH 5 (10 mM acetate buffer) containing urease ($30 \mu\text{g mL}^{-1}$) upon addition of urea (25 mM).

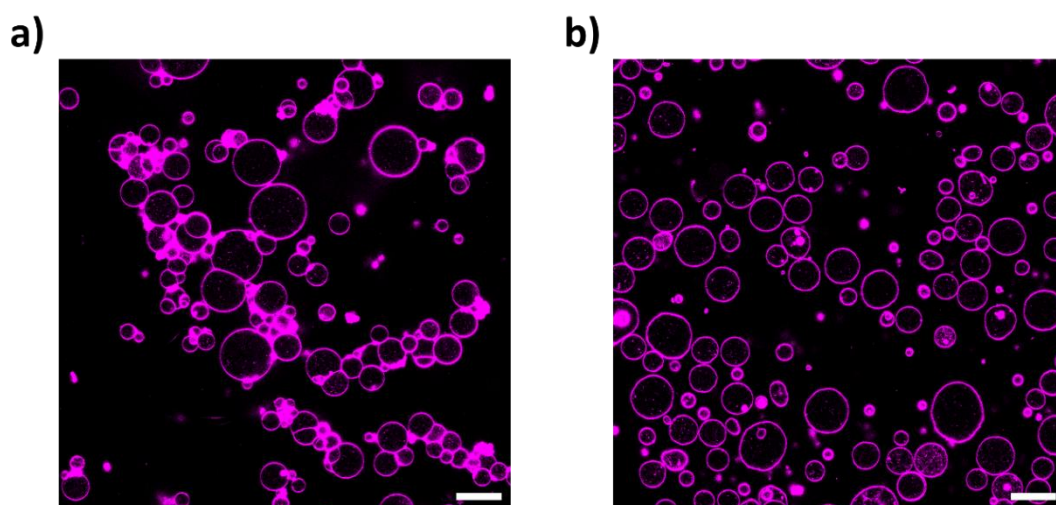


Fig. S2 a) Micrograph of GUVs containing 0% of pegylated lipid. GUVs are formed but they appear clustered. b) Micrograph of GUVs containing 1% of pegylated lipid. Scale bar=20 μm . GUVs were labelled with DOPE-RhB as membrane marker.

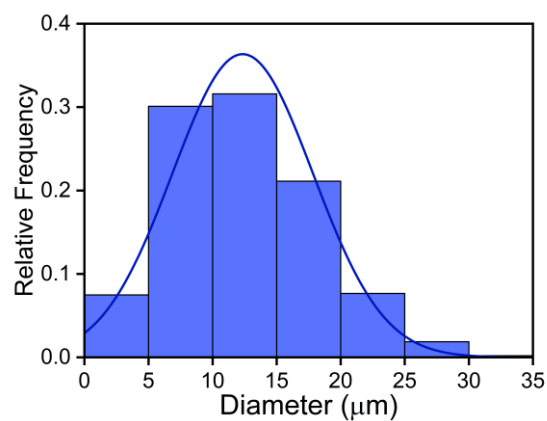


Fig. S3 Size distribution of GUVs. Data corresponds to the analysis of multiple micrographs of two independent samples (N=537).

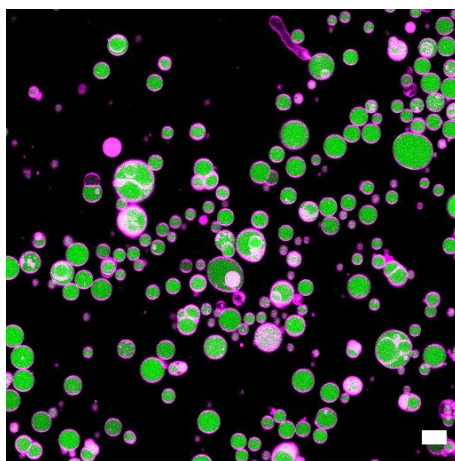


Fig. S4 Micrograph of GUVs loaded with calcein in the inner phase, confirming the encapsulation of molecular cargo and the removal of unencapsulated material from the outer phase. Scale bar=25 μm.

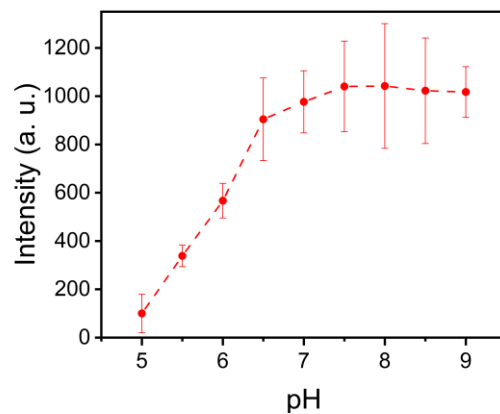


Fig. S5 GFP emission intensity in PBS buffer (1X) at different pHs. Excitation wavelength=488 nm, emission wavelength=510 nm, GFP concentration=55 ng/mL. Results are expressed as mean \pm standard deviation from 3 different samples.

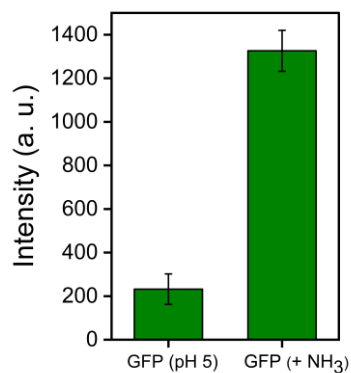


Fig. S6 GFP emission intensity in acetate buffer (10 mM) at pH 5 before (left) and after (right) addition of 5 mM NH₃. Excitation wavelength=488 nm, emission wavelength=510 nm, GFP concentration=55 ng/mL. Results are expressed as mean \pm standard deviation from 3 different samples.

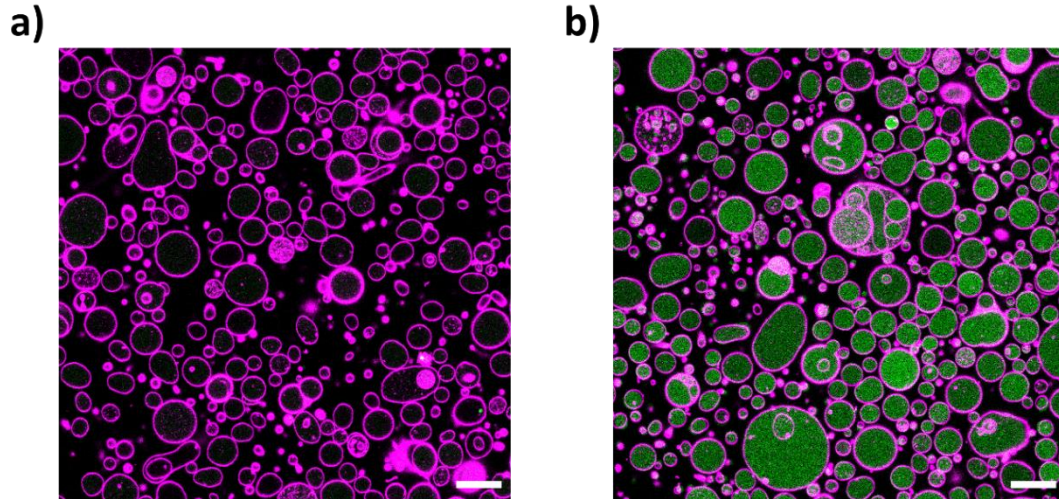


Fig. S7 Micrograph of GFP-loaded GUVs, showing membrane marker in pink and GFP signal in green: (a) as-made (10 mM acetate buffer, pH 5), and upon addition of NH_3 (5 mM). The results indicate that artificial cells are able to sense the presence of NH_3 (signalling molecule in the quorum communication system).

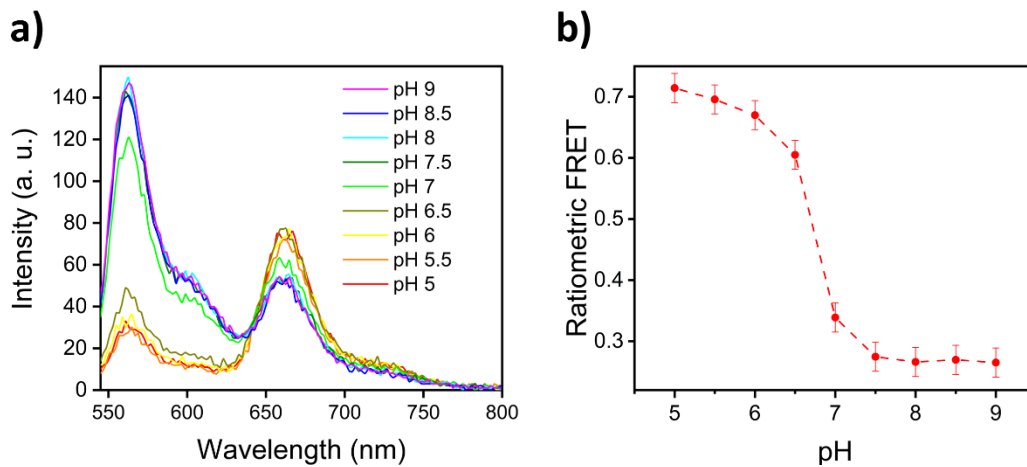


Fig. S8 Spectroscopic characterization of the pH-responsive DNA nanostructure at different pHs. Labelling with the Cy3–Cy5 FRET pair allows to monitor its structural change by fluorescence measurements: the Cy3 (located in the internal loop) and the Cy5 fluorophore (located at the 3'-end flanking tail) are in near proximity in the triplex conformation resulting in efficient energy transfer from Cy3–Cy5 (Fig 3 in the manuscript). The FRET ratio stayed approximately constant in the 5–6.5 pH range, whereas a sharp decrease was observed upon reaching pH 7–7.5, with no further changes at higher pH values (Fig. S7 a and b). This change in fluorescence is ascribed to the opening of the nanostructure at basic pH. **a)** Raw emission spectra of the pH-responsive DNA nanostructure in bulk solution (500 nM) in PBS (1X) adjusted at the

corresponding pH. It shows an increase of the Cy3 signal and a decrease of the Cy5 signal with pH, corresponding to the triplex-to-duplex transition. Excitation wavelength was 530 nm. **b)** Ratiometric FRET emission plot which indicates triplex-to-duplex transition of the DNA nanostructure as a function of pH. Ratiometric FRET was calculated as $F_{Cy5}/(F_{Cy3} + F_{Cy5})$; where F_{Cy5} is the maximum fluorescence emission of Cy5 ($\lambda_{em}=660$ nm) and F_{Cy3} ($\lambda_{em}=563$ nm).² Results are expressed as mean \pm standard deviation from 2 different samples.

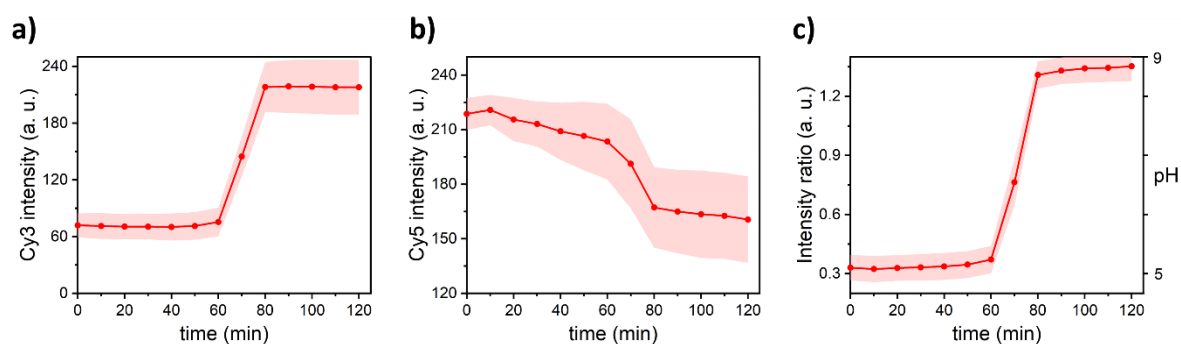


Fig. S9 Time-dependent response in urease/DNA-GUV consortia (at high cell concentration) upon addition of 25 mM of urea. (a) Fluorescence response for the Cy3 channel. (b) Fluorescence response for the Cy5 channel. (c) Quantification of Cy3/Cy5 intensity and pH change. An increase from an initial pH of 5 to ~8.8 was registered.

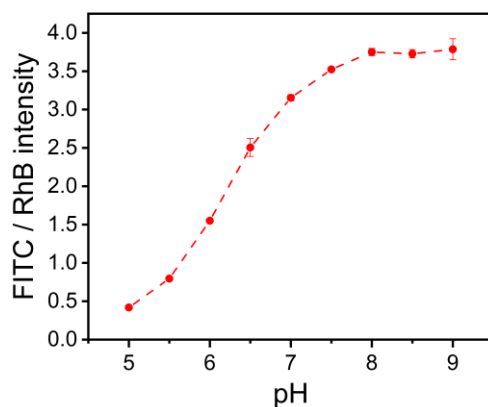


Fig. S10 FITC / RhB emission intensity ratio in PBS buffer (1X) at different pHs. Dextran-RhB-FITC was dissolved at 0.05 mg/mL. Fluorescein was excited at 488 nm and emission was collected at 525 nm. Rhodamine was excited at 550 nm and emission was collected at 570 nm. Results are expressed as mean \pm standard deviation from 2 different samples.

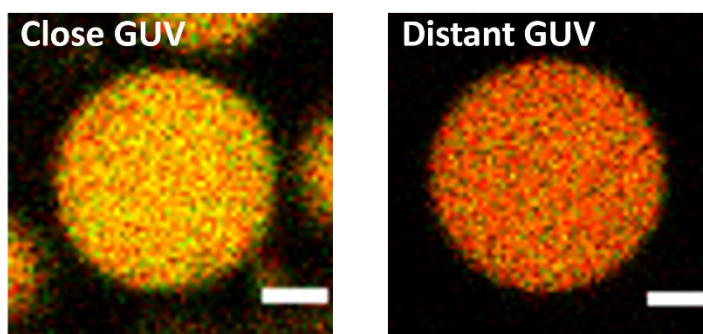


Fig. S11 Evaluation of quorum sensing depending on GUV spatial proximity. Representative micrographs showing a GUV at the edge of a highly populated cluster (close GUVs), and a GUV located further away (distant GUV) at $t=55$ min, corresponding to experiments described in Fig. 5a-b. Scale bar=10 μ m.

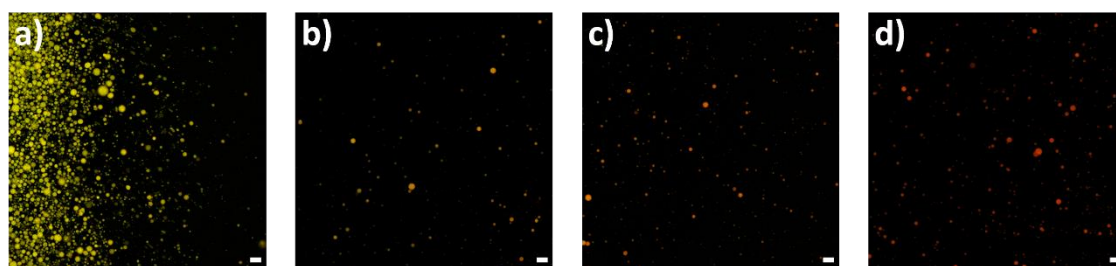


Fig. S12 Representative micrographs corresponding to different channel positions of Fig. 5c-d in the manuscript: (a) 2.1 mm, (b) 6.4 mm, (c) 8.1 mm, and (d) 12.3 mm. Full activation (yellow colored) at position a (near to the highly populated region), diminished activation in positions b and c (along the channel) and no activation (position d, red colored) at further distances. Scale bar=50 μ m.

Supplementary References

- 1 N. A. Yewdall, B. C. Buddingh, W. J. Altenburg, S. B. P. E. Timmermans, D. F. M. Vervoort, L. K. E. A. Abdelmohsen, A. F. Mason and J. C. M. Hest, Physicochemical Characterization of Polymer-Stabilized Coacervate Protocells, *ChemBioChem*, 2019, **20**, 2643–2652.
- 2 T. Patiño, A. Porchetta, A. Jannasch, A. Lladó, T. Stumpp, E. Schäffer, F. Ricci and S. Sánchez, Self-Sensing Enzyme-Powered Micromotors Equipped with pH-Responsive DNA Nanoswitches, *Nano Lett.*, 2019, **19**, 3440–3447.
- 3 B. C. Buddingh', A. Llopis-Lorente, L. K. E. A. Abdelmohsen and J. C. M. van Hest, Dynamic spatial and structural organization in artificial cells regulates signal processing by protein scaffolding, *Chem. Sci.*, 2021, **11**, 12829–12834.